European Journal of Neuroscience, Vol. 11, pp. 2635–2650, 1999 *© European Neuroscience Association*

Visual-field-specific heterogeneity within the tecto-rotundal projection of the pigeon

Burkhard Hellmann and Onur Güntürkün
Ruhr-Universität Bochum, Fakultät für Psychology, AE Biopsychologie, D-44780 Bochum, Germany

Keywords: ascending tectofugal pathway, birds, extrageniculocortical pathway, rotundus, tectum opticum, visual system

Abstract

The organization of the tecto-rotundal projection of the pigeon was investigated by means of anterograde and retrograde tracing techniques. Besides the known organization in tecto-rotundal connectivity, this study additionally demonstrates major variations in the ascending projections of different tectal subfields. We show that the ventral tectum opticum (TO) has significantly more projections onto the nucleus rotundus (Rt) than dorsal tectal areas. This difference coincides with differential innervation densities of afferent fibres within rotundal subregions. While ventral tectal efferents project onto the ventral and central Rt, dorsal tectal efferents mainly arborize within limited areas between the central Rt and its dorsal cap, the nucleus triangularis. Thus, the ventral TO, representing the lower and frontal field of view, exhibits a quantitatively and spatially enhanced projection onto the Rt, as compared with the dorsal TO. The data presented here demonstrate a visual field-dependent projection pattern of ascending tectal outputs onto different rotundal domains. The data are consistent with behavioural studies, demonstrating tectofugal lesions to suppress visual stimulus analysis mainly within the frontal field of view.

Introduction

In all amniotes studied so far, visual input ascends via two parallel pathways to the forebrain. In birds, these are the thalamo- and tectofugal pathways which are probably homologous to the geniculocortical and extrageniculocortical systems in mammals (Shimizu & Karten, 1993). Within the thalamofugal pathway, visual input is represented in the contralateral nucleus geniculatus lateralis, pars dorsalis (GLd). This nucleus predominately projects to the ipsilateral telencephalic visual wulst (Karten *et al*., 1973; Nixdorf & Bischof, 1982; Bagnoli & Burkhalter, 1983; Miceli *et al*., 1990).

In pigeons, ≈90% of the retinal ganglion cells project onto the contralateral tectum opticum (TO), the first centre of the tectofugal pathway. In superficial tectal layers, visual input is represented topographically. Neurons of the deep tectal layer 13 (nomenclature according to Ramon y Cajal, 1911) project bilaterally onto the nucleus rotundus (Rt). The Rt is connected to the ipsilateral ectostriatal core of the forebrain, from where efferent fibres ascend into the surrounding belt (Karten & Revzin, 1966; Nixdorf & Bischof, 1982; Watanabe *et al*., 1985; Bischof & Niemann, 1990; Güntürkün *et al*., 1993a).

Studies with Rt and ectostriatum lesions revealed the involvement of the tectofugal system in pattern, luminance, colour and movement discrimination in pigeons (Hodos & Karten, 1966; Hodos, 1969; Bessette & Hodos, 1989; Watanabe, 1991). Electrophysiological data on the properties of tectal and rotundal neurons are in accordance with these behavioural findings, as different aspects of visual stimuli, e.g. luminance, colour, pattern and object motion in two- and three-dimensional space are processed within the tectofugal pathway, and these different stimulus features are represented in regional subdivisions within the Rt (Granda & Yazulla, 1971; Jassik-Gerschenfeld & Guichard, 1972; Yazulla & Granda, 1973; Frost & DiFranco, 1976; Revzin, 1979; Wang *et al*., 1993).

Visually driven units within the pigeon GLd and wulst were shown to be sensitive for moving and stationary stimuli with low adaption to stimulus repetition (Britto *et al*., 1975; Jassik-Gerschenfeld *et al*., 1976; Maxwell & Granda, 1979; Miceli *et al*., 1979; Britten, 1987). In contrast to the tectofugal system, thalamofugal neurons exhibit more narrowly tuned receptive fields of partly complex shape. Therefore, Britto *et al*. (1975) suggested that the thalamofugal pathway might be involved in pattern analysis. Unfortunately, these predictions on the functional role of the thalamofugal pathway could not be confirmed in behavioural experiments yet. Lesion studies showed only minor impairments in visually related tasks, if any (Pritz *et al*., 1970; Hodos & Bonbright, 1974; Hodos, 1976; Mulvanny, 1979; Güntürkün *et al*., 1993b).

A new approach in understanding the functional architecture of the two visual pathways in birds followed the observation of regional variations in retinal output patterns. In owls and falcons as well as in the pigeon, only parts of the retina project onto the GLd (Bravo & Pettigrew, 1981; Bravo & Inzunza, 1983; Remy & Güntürkün, 1991). In the pigeon, the retina has two regions of enhanced ganglion cell density: the central fovea receives input from the lateral field of view, while the area dorsalis, which is located within the superior-temporal retina, processes stimuli in the frontal visual field (Hayes *et al*., 1987). While the central fovea is strongly represented within the thalamofugal pathway, only a few retinal ganglion cells of the area dorsalis innervate the GLd (Remy & Güntürkün, 1991). Therefore, the authors suggested the thalamofugal pathway to be specialized for lateral visual field analysis. Recent behavioural studies support this view demonstrating visual field-dependent processing within the two ascending visual pathways. GLd lesions cause massive impairments in acuity performance exclusively in the lateral visual field, while

Correspondence: Dr B. Hellmann, as above.
E-mail: burkhard.hellmann@ruhr-uni-bochum.de

Received 26 August 1998, revised 18 March 1999, accepted 22 March 1999

rotundal lesions lead to similar effects in spatial resolution performance restricted to the frontal field of view (Güntürkün & Hahmann, 1998). With regard to the thalamofugal pathway, the behavioural data are in accordance with the specific pattern of sensory input. However, these findings on visual field-dependent processing raise new questions about the functional organization within the tectofugal pathway.

Because the frontal as well as the lateral visual field are represented within the TO, it could be expected that deficits in lateral acuity after GLd lesions are compensated for by tectofugal mechanisms. However, behavioural compensation could not be observed (Güntürkün & Hahmann, 1998). Taken together with the behavioural effects of Rt lesions which are limited to frontal acuity performance, the data suggest a visual field-specific mode of processing in the tectofugal system. The retino-tectal projection is organized topographically, in that the superio-temporal retina, including the area dorsalis, projects onto the rostro-ventral TO, while the central retina is represented at the lateral tectal pole (Hamdi & Whitteridge, 1954; Jassik-Gerschenfeld & Hardy, 1984; Remy & Güntürkün, 1991).

With this background of behavioural data, it is conceivable that the organization of the tecto-rotundal projection differs for tectal areas representing different fields of view. To test this hypothesis, we analysed the tecto-rotundal system using anterograde and retrograde neuronal tracers.

Materials and methods

Surgery and preparation

Sixty-four adult pigeons (*Columba livia*) of unknown sex from local breeding stocks were used in this study. Fifty-eight animals received injections of tracers into the tectum. To confirm the anterograde tracing data, six animals were injected with retrograde tracers into the Rt. All experiments were carried out according to the specifications of the German law for the prevention of cruelty to animals.

Prior to surgery, the pigeons were anaesthetized with equithesin (0.33 mL per 100 g body weight), and the animals were placed into a stereotaxic apparatus (Karten & Hodos, 1967). For tectal tracer injections, a modified device was used which allowed lateral rotation of the head along the longitudinal axis over 100° to the left and right. The scalps were infiltrated with xylocaine, and subsequently incised either between eye and ear hole (tectal injections) or dorsally (rotundal injections). Next the scull was opened with a dental drill, and a glass micropipette (outer tip diameter 20–25 µm) mounted to a mechanic pressure device (WPI Nanoliterinjector, WPI, USA) was inserted into the Rt or the deep tectal layers according to stereotaxic coordinates of the pigeon brain atlas by Karten & Hodos (1967). The different tracers were injected in steps of 2 nL over a period of 20–30 min. Subsequently, the pipette was removed and the skin was infiltrated again with xylocaine and sutured.

After survival times ranging from 30 h to 10 days, depending on the tracer used, the animals received an injection of 200 units sodium heparin and were then deeply anaesthetized with an overdose of equithesin (0.55 mL per 100 g body weight). The pigeons were perfused through the heart with 100 mL 0.9% (w/v) sodium chloride and 800 mL ice-cold 4% paraformaldehyde in 0.12 M phosphate buffer (PB), pH 7.4. The brains were removed and stored for 4 h in fixative with supplement of 15% sucrose (w/v). Subsequently, the brains were stored overnight in a solution of 30% sucrose in 0.12 M PB. On the following day the brains were cut in the frontal plane at 35 µm on a freezing microtome and the slices were collected in PB containing 0.1% sodium azide (w/v).

Tracers and their histochemical demonstration

Five different tracers were used in the experiments. Four of them were lysine-coupled dextranamines (Molecular Probes, Leiden, The Netherlands), additionally, choleratoxin subunit B (CtB) was used (Sigma, Deisenhofen, Germany). Most tectal injections were carried out with biotinylated dextran amines (BDA) with molecular weights of 3000 or 10 000 MW. For double-labelling experiments with tracer injections into the dorsal as well as the ventral tectum, Texas Red dextran amine- (TDA) and fluorescein dextran amine- (FDA) labelled dextrans with 10 000 MW were used. Either BDA (10 000 MW) or CtB was injected into the nucleus rotundus.

All dextrans were pressure injected as 8% (FDA) or 12% (BDA, TDA) solutions (w/v) in 0.12 M phosphate-buffered saline (PBS) with an addition of 2% dimethylsulphoxide. The injection volume ranged from 60 to 120 nL (tectal delivery) or 40–60 nL (Rt). The animals were killed after survival times of 1–10 days (8 days being most common). CtB was injected as a 1% solution (w/v) in distilled water. Applied volumes ranged between 20 and 40 nL. The survival times were 48–72 h.

The cryosectioned brain slices of animals that had received fluorescent tracer injections were mounted on gelatine-coated slides, air-dried and coverslipped with Fluoromount (Serva, Heidelberg, Germany) or ProLong Antifade Kit (Molecular Probes). Sections were viewed with an Olympus BH2 epifluorescence microscope with the following filter settings. FDA: Olympus IB-set with additional shortpass emission filter G520, TDA: Chroma filters (Brattleboro, USA) with excitation filter HQ-577/10, dichroic mirror Q-585LP and emission filter HQ-645/75.

Brain slices containing BDA were reacted free-floating according to the streptavidin–peroxidase technique. The sections were placed for 35 min in 1% hydrogen peroxidase/50% ethanol to reduce endogenous peroxidase activity. After rinsing, slices were incubated for 60 min in streptavidin solution at room temperature [Jackson, West Grove, USA; 1/800 in 0.12 M PBS with the addition of 1.1% NaCl (w/v) and 0.3% Triton X-100 (v/v)]. After additional rinsing, the peroxidase activity was detected using a heavy metal-intensified 3,3′-diaminobenzidine (DAB; Sigma) reaction (Adams, 1981), modified by the use of β-D-glucose/glucose-oxidase (Sigma) instead of hydrogen peroxidase (Shu *et al.*, 1988). The sections were mounted on gelatine-coated slides, dehydrated and coverslipped with DPX (Fluka, Neu-Ulm, Germany) or Permount (Fisher Scientific, New Jersey, USA). Some sections were counterstained with cresyl violet.

CtB-labelled sections were reacted free-floating according to the immuno-ABC technique. After reduction of endogenous peroxidase activity (see above), sections were incubated overnight at 4 °C in the primary antibody [goat anti-choleragenoid; Camon, Wiesbaden, Germany; 1/20 000 in 0.12 M PBS after the addition of 1.1% NaCl (w/v), 0.3% Triton-X 100 (v/v) and 5% normal rabbit serum]. After being rinsed, the sections were incubated for 60 min at room temperature in the biotinylated secondary antibody (rabbit antigoat; Vectastain, Vector, Camon, Wiesbaden, Germany; 1/500 in 0.12 M PBS + 1.1% NaCl + 0.3% Triton X-100). After additional rinsing, the sections were incubated for 60 min in avidin–biotin–peroxidase solution (Vectastain ABC-Elite kit, Vector; 1/100 in 0.12 M PBS + 1.1% NaCl + 0.3% Triton X-100). After washing, a heavy metal-intensified DAB reaction was performed, and slices were mounted and coverslipped (see BDA section).

Evaluation

The tracer injection sites and the resulting neuronal labelling were reconstructed using an Olympus BH2 microscope. Structures were drawn using PC software Designer 3.1 (Micrografx, USA). Often a digitized picture of the section was displayed on a second computer monitor, using a b/w video camera (Kappa CF 8, Gleichen, Germany) attached to the microscope and PC-based computer hardware configuration (Soft Imaging System, Münster, Germany). Photographic documentation was carried out with a 35-mm camera system attached to the microscope using Agfa APX 25, Ilford HP5, Agfa RSX 50 or Kodak Ectachrome 200 films.

After some tectal BDA injections, three-dimensional reconstructions of variations in intrarotundal labelling intensities were carried out with the image analysis systems 'analySIS' and '3dSIS' (SIS, Münster, Germany). For this purpose, images of every third section of the ipsilateral Rt were digitized. After additive shading correction using a correction image without specimen, rotundal labelling intensities were normalized by subtracting the average grey level of non-specific background labelling from every image. Subsequently, the grey levels of both weak and strong intrarotundal labelling were determined for every section as the average of three measurements. The threshold between differently labelled rotundal areas was defined as the mean of these two grey values, and the Rt was subdivided into regions of either low or high fibre densities. Finally, subdivisions were reconstructed as three-dimensional models.

Quantitative analyses of anterograde rotundal fibre densities were performed in 21 animals which received tectal BDA injections with postoperative survival times ranging from 8 to 10 days. The number of labelled layer 13 neurons was estimated by counting the DAB-labelled cells in Nissl-counterstained sections of the TO. Every third section of the TO was used. To quantify the amount of anterograde axonal labelling within the Rt (ipsilateral to the tracer injection site), five randomly chosen areas of three different sections along the rostro-caudal axis of the ipsilateral Rt (A5.75, A6.25 and\ A6.75 according to the pigeon brain atlas by Karten & Hodos, 1967) were quantified. This was done with an ocular micrometer-plate (10×10 mm) with 10 horizontal and 10 vertical subdivisions of 1 mm distance at a magnification of $\times 1250$, resulting in a measurement area of 64 μm^2. The crossing points of micrometer-plate subdivisions with labelled intrarotundal axonal processes were counted, and the average of the 15 measurements per animal was multiplied by 100 and divided by the estimated total number of retrogradely labelled layer 13 cell bodies within the TO (density index).

Reconstruction of tectal tracer injection sites or retrogradely labelled tectal somata after rotundal BDA applications was performed on a two-dimensional reconstruction of tectal layer 13 surface.

Results

Tectal tracer injections

The nucleus rotundus is the largest cellular complex within the thalamus of the pigeon. It extends over a rostro-caudal distance of almost 2 mm (A5.3–A7.2) in the central to lateral aspects of the thalamus. In Nissl-stained material, the Rt is easily distinguishable from neighbouring cell groups by the presence of big ovoid to round neuronal somata. These principal neurons (Figs 1 and 2a; mean diameter of 22 μm in DAB/cresyl violet double-labelled frozen sections) are distributed throughout its entire extent. They are also common in the nucleus triangularis (T), which is located dorso-medial to Rt (Fig. 1).

Focal BDA injections into different sites of the deep layers of the TO frequently resulted in anterograde labelling of axonal processes throughout the ipsi- and contralateral Rt and T. Within the TO, fibres ran within layers 13 and 14 before they entered the brachium where they ascended rostrally. At caudal and medial rotundal levels, the axons took a more and more dorsal route, to enter the Rt ventrally. Fibres arborizing within T ran along the lateral borders of the Rt and entered the T either from its lateral or medial margin. Within the Rt and T, thick tecto-rotundal fibres ran in bundles of up to 10 axons. They often gave rise to perpendicularly orientated collaterals. Thin axonal branches with terminal-like swellings were frequently arranged within restricted areas, each receiving input from several axon collaterals. In cresyl violet-counterstained sections, these termination areas were surrounded by four to 10 rotundal neurons with a mean diameter of 22 μm (Fig. 2a). Thin fibres with terminal-like swellings were never seen to enclose somata of rotundal neurons (Fig. 2a and b).

Although tracer injections into the tectum always resulted in fibre as well as terminal-like labelling throughout nearly the entire ipsilateral Rt and T, profound variations in intrarotundal labelling intensity were observed. Two different patterns could be distinguished (Fig. 3).

Irrespective of their rostro-caudal placement, tracer injections situated in the ventral third of the TO resulted in labelling of a dense fibre network within the ventral half of the Rt along almost its entire rostro-caudal extent. The most caudal region was spared in its peripheral aspects (A5.30–A5.50). The region adjoining directly rostrally received a reversed termination pattern with high fibre densities in the marginal rotundal aspects, sparing a dorso-lateral and central area. The dorsally adjoining T exhibited strong labelling within its ventral, medial and dorsal regions, while the central and lateral aspects were spared. At rostro-caudal levels between A5.7 and A6.35, the rotundal area of high fibre and terminal densities gradually increased in that the borderline to regions of weak label shifted more and more centrally and then dorsally. The T extends rostrally up to A6.5. A gradual increase of fibre density was obvious within the dorso-lateral division. The central T remained weakly labelled with the exception of small spots of extremely high termination densities at A6.0. Within the rostral Rt (A6.5–A7.2), ventrally located tectal BDA injections resulted in a comparatively homogeneous tracing pattern with generally high fibre densities. Tectal input slightly declined within the dorsal Rt. This was apparent in the sharp medio-laterally arranged borderline between differing termination densities within the rostral Rt (Fig. 4).

The second rotundal labelling pattern resulted from tracer injections into the lateral and dorsal TO. Again, no variations were observed depending on the rostro-caudal extent of the tectal injection site. The intrarotundal labelling pattern was roughly opposite to that observed after ventral tectal applications. High fibre densities were present within the most caudal 250 μm of the Rt, where only a central part of the Rt was spared. More rostrally, but within the caudal two-thirds of the Rt, overall fibre densities decreased. Strong labelling was restricted to a medio-laterally arranged band with decreasing thickness from lateral to medial. While the most dorsal aspects of the Rt received weak input from the dorsal tectum, high fibre and termination densities occurred within the ventro-lateral and the most dorsal regions of the T. In all other regions, including the entire rostral third of the Rt, only very few fibres and terminal-like swellings were observed. The two different anterograde labelling patterns were

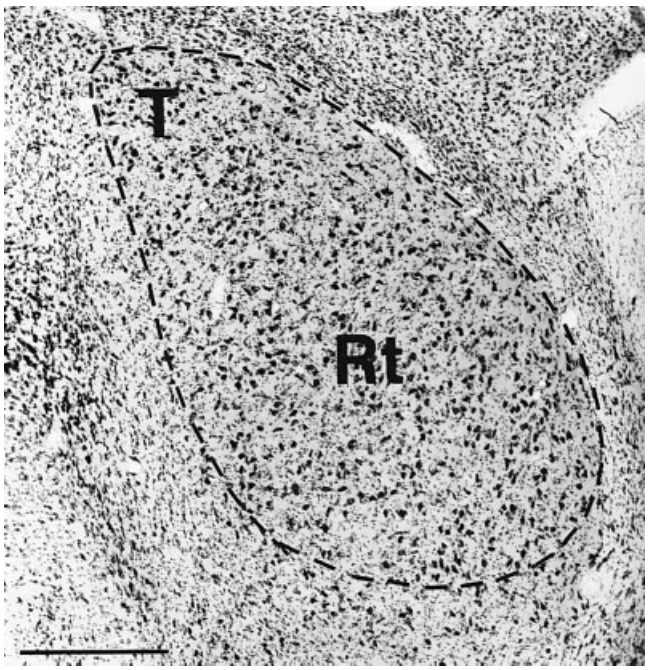

FIG. 1. Cresyl violet-stained transversal section of the pigeon thalamus at A5.9 (Karten & Hodos, 1967) with Rt and the dorso-medially adjoining T. Both nuclei are easily distinguishable from surrounding tissue by the occurrence of big ovoid to round somata. The extension of both nuclei is indicated by the stippled line. Bar, 500 µm.

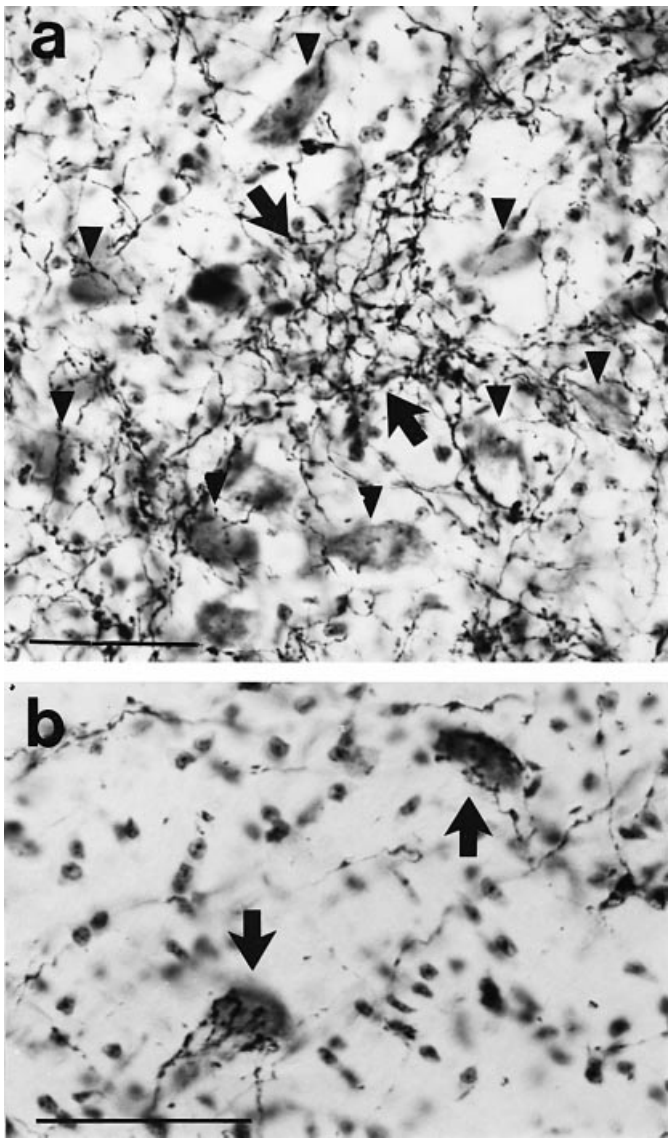

FIG. 2. (a) Section of the nucleus rotundus after injection of BDA into the ipsilateral ventral tectum opticum. Thin axonal processes with terminal-like swellings were frequently arranged as rotundal fibre webs (arrows), innervated by several tecto-rotundal axons and surrounded by cresyl violet-stained principal neurons (arrowheads). Axosomatic contacts as seen in the neighbouring nucleus posteroventralis thalami (PV; b) were not observed. Bar, 50 µm. (b) In contrast to Rt, within the medially adjoining PV, fine sidebranches of ascending tectal axons often surrounded somata of PV neurons (arrows). Bar, 50 µm.

accompanied by characteristic regional variations in rotundal fibre densities (Fig. 5).

Double injections of TDA and FDA into the dorsal and ventral TO revealed an intrarotundal segregation of ventral versus dorso-lateral tectal projections onto the Rt (Fig. 6a and b). Regions of enhanced dorsal tectal projections received comparatively weak input from the ventral TO. Only in the most dorsal regions of the rostral T did relatively high densities of both tracers seem to intermingle (Fig. 7a and b).

Beyond these regional variations in tecto-rotundal connectivity, overall rotundal projections of the lateral and dorsal TO were significantly weaker compared with those of the ventral TO ($P < 0.001$, $n = 21$, $Z = 3.873$, Mann–Whitney test). The fibre density index indicated a 15-fold increase of anterogradely labelled rotundal fibres per layer 13 neuron after ventral tectal BDA injections (Fig. 8).

Projections of the ventral TO onto the contralateral Rt and T were generally less numerous compared with ipsilateral labelling. Aside from this quantitative difference, intrarotundal segregation in termination density corresponded with the ipsilateral variation. After dorsal and lateral tectal tracer placements, labelling within the contralateral Rt was observed in only nine out of 19 animals. In four cases, traced fibres were restricted to the caudo-lateral Rt. The remaining five pigeons exhibited similar regional variations in fibre density within the ipsi- and contralateral Rt.

Rotundal tracer injections

Injections of BDA and CtB into the Rt resulted in retrograde labelling of somata within both tecta predominantly ipsilateral to the injection site. The great majority of neurons were located within tectal layer 13. Few additional cells were traced within layers 6–12. Generally, CtB injections resulted in labelling of 15 times more somata than BDA injections. Moreover, lateral and radial dendritic processes of layer 13 neurons were filled over long distances only after CtB injections (Fig. 9a and b).

Irrespectively of the tracer in use, a dorso-ventral shift in the number of retrogradely labelled cells occurred. The highest cell numbers were counted within the ventral third of tectal layer 13, containing on average 52.5% of all labelled tecto-rotundal neurons, 18.9% of labelled cells were located within the dorsal third (Fig. 10).

The relative amount of tectal cells labelled within the ventral third ranged from 43.3 to 64.9% (Fig. 11). The lowest proportion of ventrally located layer 13 neurons was observed within the two animals which exhibited predominantly dorsal and latero-central rotundal tracer spread (both 43.3%). In contrast, more ventrally or rostrally situated injections resulted in enhanced proportions of

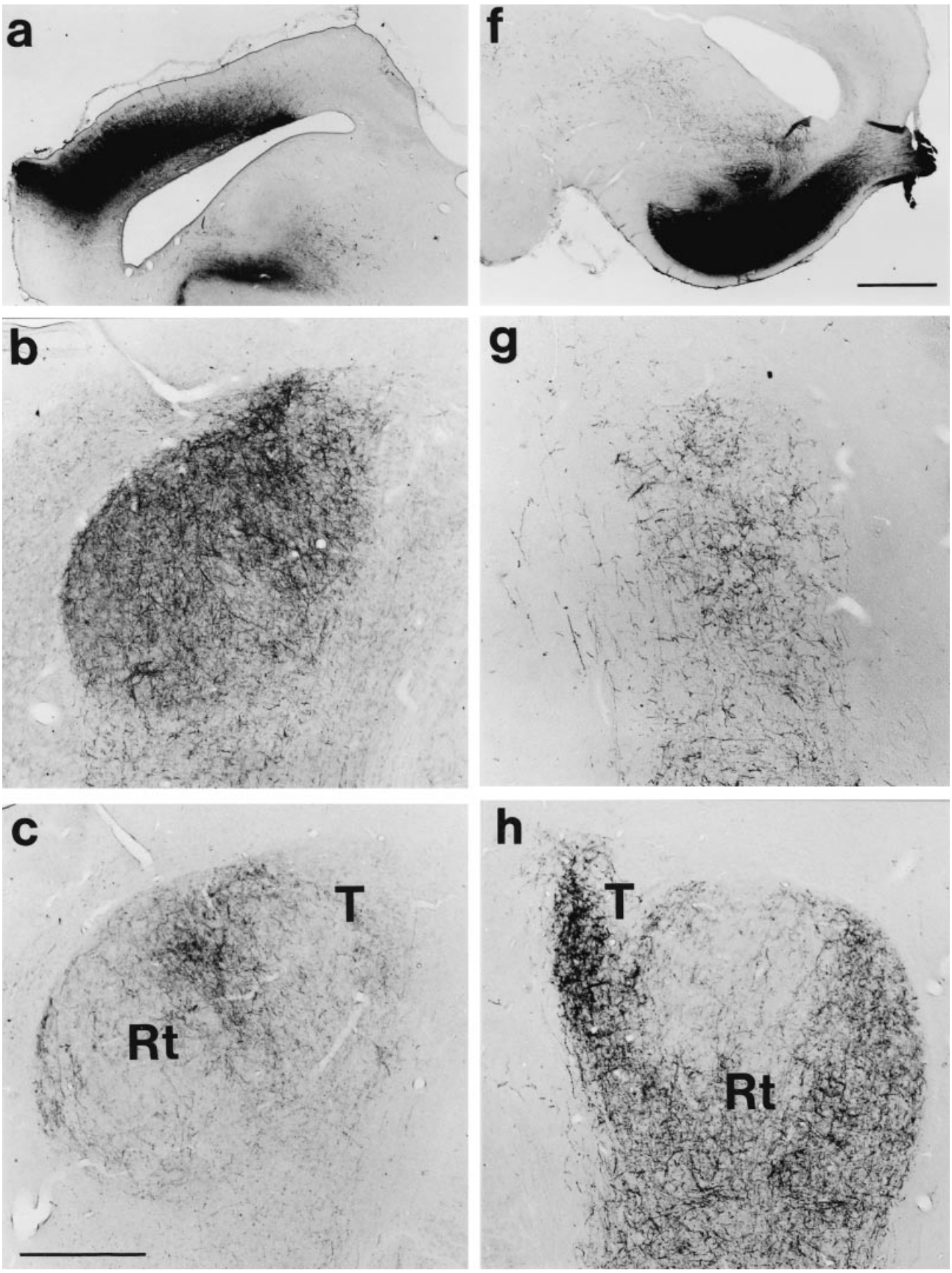

FIG. 3. Continued overleaf

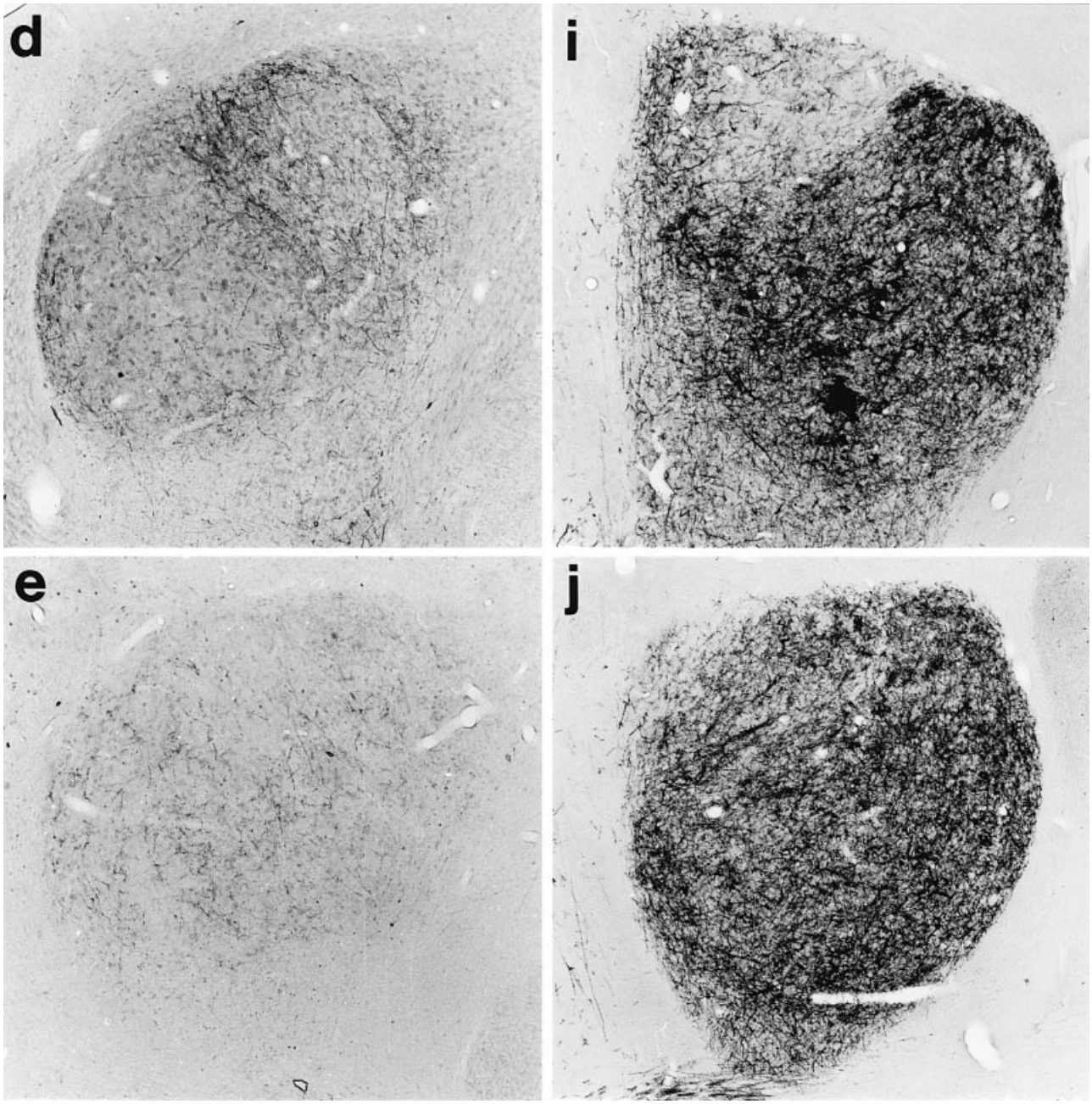

FIG. 3. (a–j) Transversal sections through TO (a and f) and Rt (b–e and g–j) after BDA injections into the dorsal (a–e) and ventral TO (f–j). On the top of each column, tracer injection sites are shown either within the dorsal (left, a) or ventral TO (right, f). Bar, 1000 μm. Below each tectum, four photographs represent the resulting anterograde fibre labelling within Rt and T from caudal to more rostral diencephalic levels (b and g: A5.3; c and h: A5.8; d and i: A6.1; e and j: A6.5). Bar, 500 μm.

retrogradely labelled ventral layer 13 neurons (51.0–64.9%, mean 57.2%).

Besides this dorso-ventral shift in relative cell number, retrogradely labelled tectal cells varied with respect to their position in different depths of layer 13 as well as their dendritic ramifications within the outer retinorecipient layers. Rostro- and caudo-ventral rotundal CtB injections resulted in labelling of somata located mostly within the outer layer 13 and strong dendritic labelling within layer 5 (Fig. 12a and c). In contrast, dorso-lateral CtB injection resulted in a heterogeneous distribution of somata in different depths of layer 13 (Fig. 12b). Dendritic labelling was densest within layer 4, while layer 5 exhibited negligible labelling (Fig. 12d).

In three cases with rotundal BDA injections, the relative position of labelled tecto-rotundal neurons was mapped onto a two-dimensional reconstruction of the layer 13 surface. This was done independently for cells in three different depths of layer 13 by estimating the radial extension of layer 13 using differential interference contrast, as no cresyl violet counterstain was performed because of the weak labelling intensity of BDA-labelled somata (Fig. 9b). A sublamina-specific distribution of cell bodies was observed (Fig. 13). Somata within the inner layer 13 were always concentrated in the ventral half, while intermediate and outer layer 13 neurons showed a variable distribution within the ventral, rostral or dorsal TO, depending on rotundal application site.

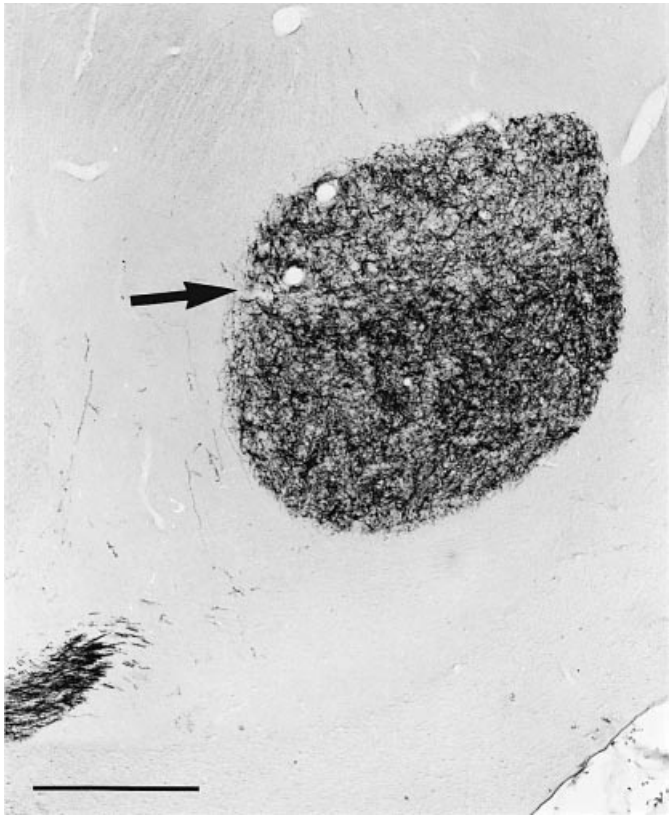

FIG. 4. Distribution of anterogradely labelled fibres within the rostral Rt (A6.8) after BDA injection into the ventral tectum. Dorsal areas exhibit slighter fibre densities than ventral regions. Arrow points to the transition zone. Bar, 500 μm.

Besides retrograde labelling of tectal layer 13 neurons, rotundal tracer injections labelled fibres within the contralateral Rt. These fibres displayed a regional distribution which reflected exactly the extent of tracer spread within the injected Rt.

Discussion

The present study shows that the tecto-rotundal projection of the pigeon is much more heterogeneous than previously known. Although all regions of the TO participate in processing ascending tectofugal information, the projection of the dorsal TO is much weaker compared with the ventral TO. Moreover, dorsal and ventral TO exhibit regional variations in their termination densities within different rotundal and triangular subdivisions.

The Rt, together with its dorsal cap, the T, is the most extensive nuclear complex in the thalamus of birds. Golgi studies have shown two different types of rotundal neurons. Besides the small GABAergic interneurons, nearly 95% of the cells are of the big multiangular type (Tömböl *et al*., 1992). These cells are the source of the ascending telencephalic projection within the tectofugal pathway (Karten & Hodos, 1970; Hunt & Künzle, 1976; Nixdorf & Bischof, 1982; Bagnoli & Burkhalter, 1983, 1990). In chicks, several rotundal relay neurons develop extensive dendritic ramifications within common 'termination fields', where they probably receive axo-dendritic input via the ascending tectal projection (Thin *et al*., 1992; Ngo *et al*., 1994). Tectal BDA injections resulted in labelling of axonal processes within the entire Rt. In regions of high fibre densities, thin fibre processes and terminal-like swellings were clustered in restricted areas of the intercellular space, surrounded by rotundal relay neurons. Each cluster received input from several axonal processes as it was shown for the termination fields in chicks. It is very likely that these anterogradely labelled rotundal termination clusters match with the termination fields of rotundal relay neurons shown in golgi studies. These data indicate two different principles in the connectivity of tectal layer 13 and rotundal relay neurons, as previously suggested by Tömböl *et al*. (1992). (i) As each termination field receives input from several axonal processes, each field seems to integrate input from different layer 13 neurons, indicating convergence of afferent information flow. (ii) As several rotundal relay neurons share access to this input within a given termination field, afferent input seems to diverge onto different rotundal cells. This arrangement of divergence and convergence in tecto-rotundal connectivity might be further complicated by the assumption that dendritic processes of individual relay neurons contact different termination fields, and axon collaterals of individual layer 13 neurons could also innervate several termination areas (Tömböl *et al*., 1992). Termination fields were labelled throughout the entire Rt, suggesting that the basic characteristics of the tecto-rotundal connectivity pattern are common to different intrarotundal functional domains, observed in electrophysiological studies (Maxwell & Granda, 1979; Revzin, 1979; Wang *et al*., 1993).

Topology of the tecto-rotundal projection

Several studies demonstrated intrarotundal differentiations on the basis of histochemical (Martinez-de-la-Torre *et al*., 1990) electrophysiological and tract-tracing techniques. Benowitz & Karten (1976) were the first to describe the topographic nature of the tectofugal pathway in the pigeon, based on horseradish peroxidase (HRP) injections into Rt and ectostriatum. T and subdivisions of the Rt receive input from neurons of different depths within tectal layer 13 and, in turn, project onto restricted regions of the ectostriatum. The present study supports this view, as the depth of retrogradely labelled layer 13 somata varied with rotundal tracer injection site. A similar pattern of connectivity was shown for zebra finches and chicks, subdividing Rt into posterior, medial, ventral and anterior-dorsal divisions (Nixdorf & Bischof, 1982; Deng & Rogers, 1998).

Depending on their depth location in tectal layer 13, neurons exhibit characteristic morphological features including varying dendritic termination patterns in different retinorecipient layers of the outer TO (Luksch *et al*., 1998). In pigeons, two populations of tectal layer 13 neurons were shown to exhibit distinct dendritic ramifications (Karten *et al*., 1997). Dendrites of type I neurons ramify within retinorecipient layer 5, while distal processes of type II neurons end up in layer 8 and probably receive no direct input from retinal ganglion cells. Furthermore, the present study demonstrates the existence of a third type of layer 13 neurons projecting to Rt. These neurons are characterized by their dendritic branching within tectal layer 4 (Fig. 12). A similar cell type was previously shown in the chick (Luksch *et al*., 1998). As dendritic labelling within tectal layer 4 occurred exclusively after dorso-lateral rotundal tracer injections, we conclude that type III cells are also specified with regard to their ascending projection onto a defined rotundal subdivision. A similar specification of rotundal target regions was shown for type I and II neurons (Karten *et al*., 1997). Combining these data with those from electrophysiological studies revealing different functional domains within the Rt (Maxwell & Granda, 1979; Revzin, 1979; Wang & Frost, 1992; Wang *et al*., 1993), we assume that within the tectofugal pathway, different aspects of visual information are processed in parallel functional channels (see also Deng & Rogers, 1998). Moreover, on the basis of corresponding

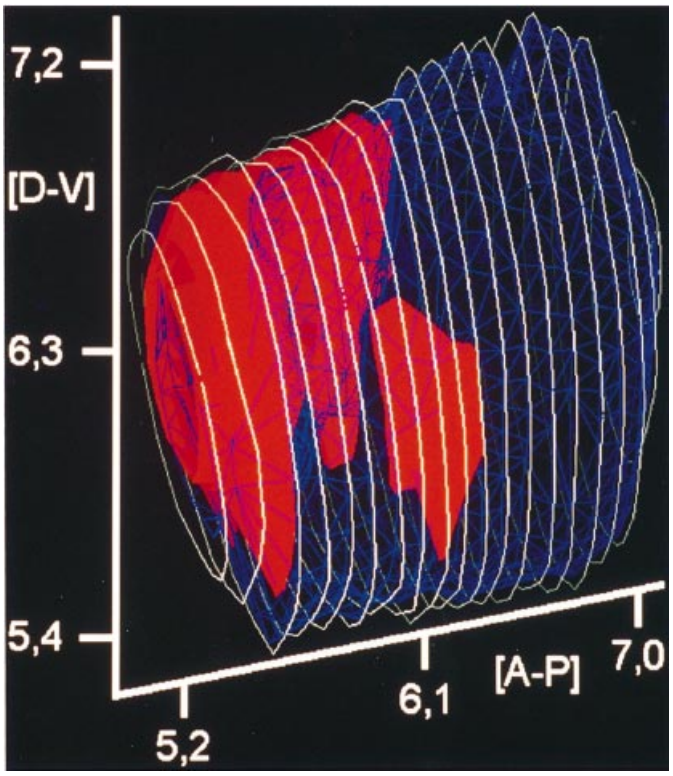

FIG. 5. Three-dimensional reconstruction of the regional distribution of dorsal (solid red areas) and ventral tectal projections (blue grid) within Rt (white lines). A–P, anterior-posterior axis; D–V, dorso-ventral axis. Numbers indicate coordinates of the pigeon brain atlas. View from the midline. For details of the reconstruction see Materials and methods.

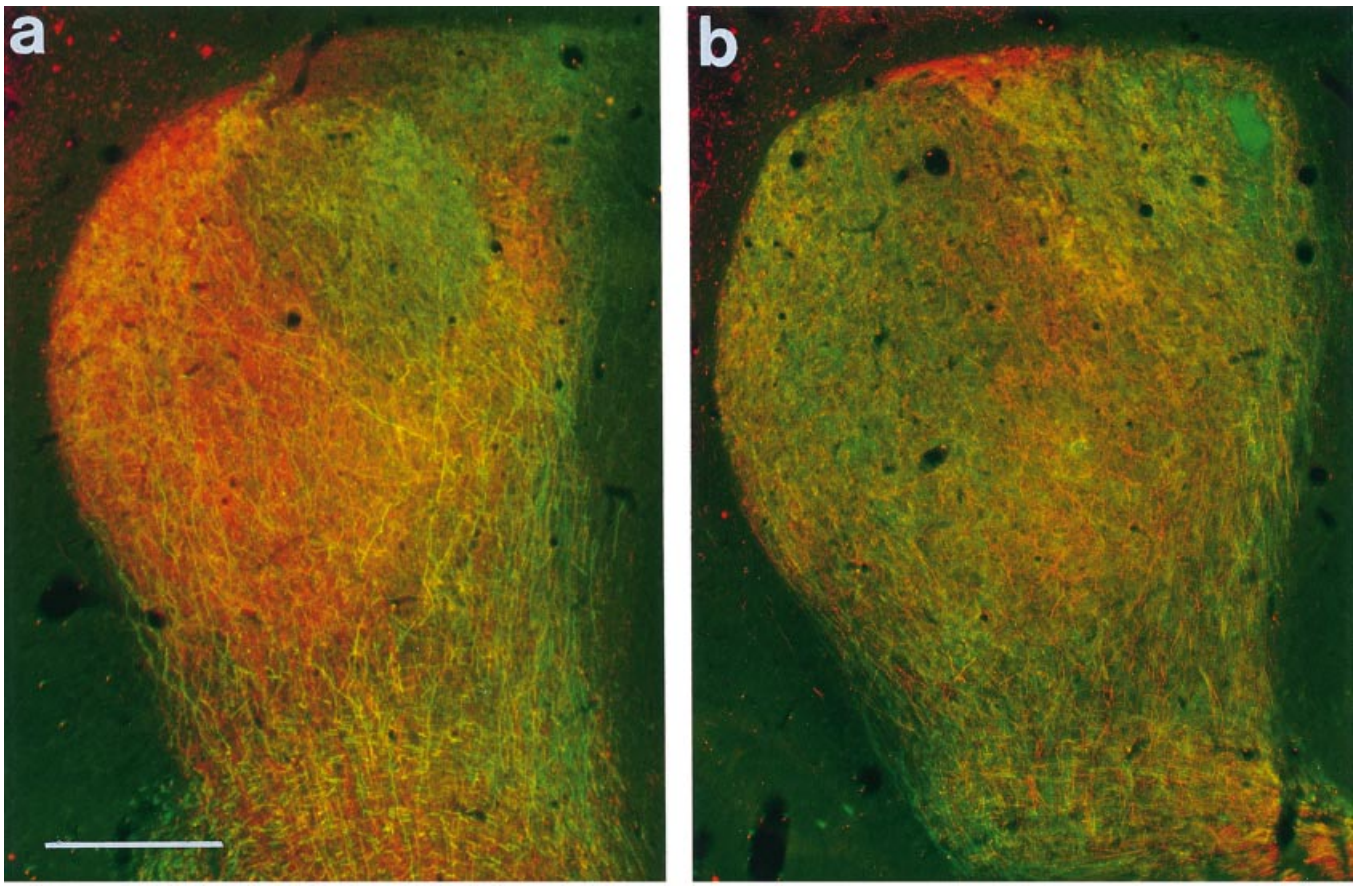

FIG. 6. Distribution of anterogradely labelled axonal processes within the caudal (a: A5.3) and central (b: A6.0) Rt after TDA injection into the dorsal (red) and FDA injection into the ventral (green) left TO. Dorsal and ventral tectal projections exhibit intrarotundal variations in labelling densities with only minor overlap of dorsal and ventral tectal projection sites (yellow). Bar, 500 µm

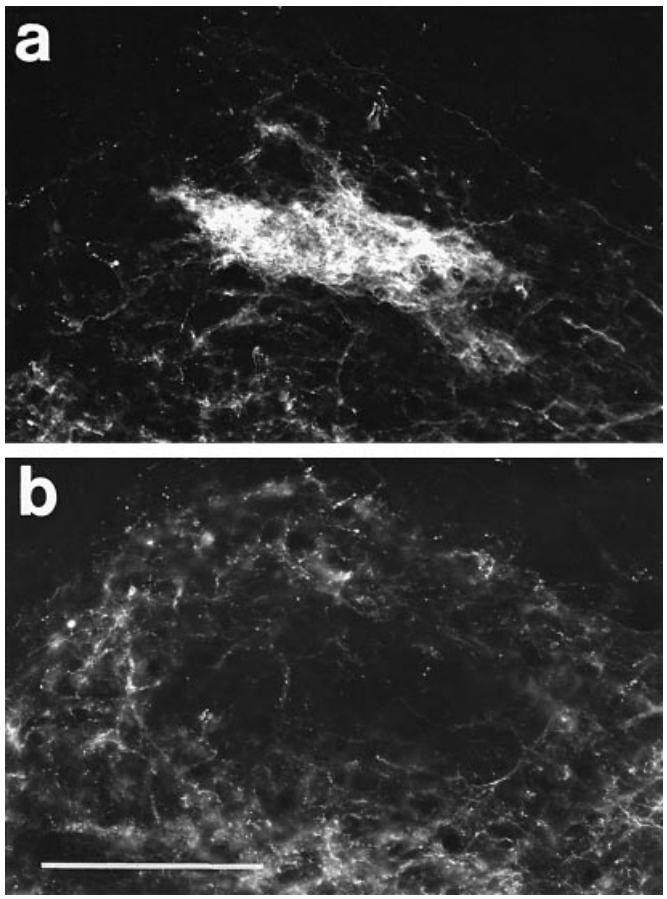

FIG. 7. Distribution of anterogradely filled fibres within the T (A6.1) of an animal which received FDA injections into the ventral and TDA injections into the dorsal tectum. Note the regional increase of projections from the ventral TO (a, FDA), which is surrounded by less intense projections from the dorsal TO (b, TDA). Bar, 200 µm.

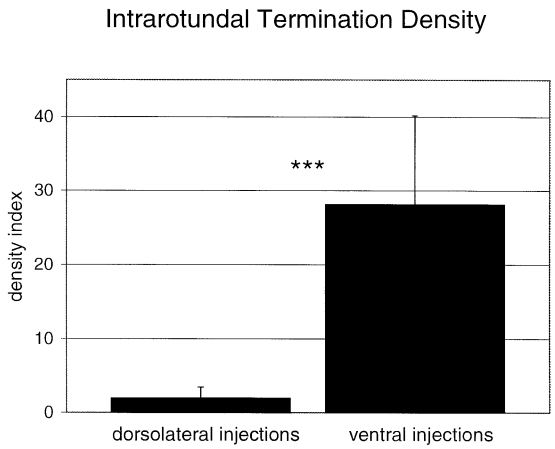

FIG. 8. Comparison of the intrarotundal fibre densities after dorsal ($n = 11$) versus ventral ($n = 10$) tectal BDA applications. The density index was calculated for each animal as the average number of fibres within 15 rotundal measurement regions multiplied by 100 and divided through the estimated number of labelled tectal layer 13 neurons (see also Materials and methods). Bars, standard deviations. Ventral tectal BDA applications resulted in 15 × higher intrarotundal fibre densities as compared with dorsal injections.

findings on the topography of the tecto-rotundal connectivity pattern in different avian species, we suggest that this organization reflects a fundamental differentiation within the tectofugal pathway at least in granivorous birds.

The main finding of the present study is that supplementary to the above-mentioned specification in tecto-rotundal connectivity, an additional topography is obvious in the tecto-rotundal projection of the pigeon. After tectal BDA injections, two different anterograde labelling patterns were observed within the Rt. Ventral tectal BDA injections resulted on average in a 15-fold overall increase in anterogradely labelled intrarotundal fibre densities (Fig. 6), compared with dorsal or lateral tectal injections. This difference was accompanied by characteristic regional variations in rotundal fibre densities. Typically, rotundal areas with strong input from the ventral TO received comparatively weak projections from the dorsal TO and vice versa, indicating rotundal domains with predominantly ventral or dorsal tectal input. Because the rostro-caudal extent of tectal tracer injection site apparently did not cause variations in intrarotundal labelling pattern, the two different tectofugal projection patterns do not correspond directly to the tectal representation of specified retinal areas, e.g. the area dorsalis or fovea centralis (Hamdi & Whitteridge, 1954; Remy & Güntürkün, 1991), but they point to a fundamental dorso-ventral differentiation in tectofugal information processing.

Meanwhile, there is a broad database concerning morphological and cytoarchitectonic peculiarities as well as differential connectivity patterns of the dorsal and ventral TO in the pigeon. The two regions differ in their contribution to centrifugal visual information processing (Woodson *et al*., 1995), their connectivity pattern with the pretectal nuclear complex (Gamlin *et al*., 1996) and their projections onto the thalamofugal GLd of the dorsal thalamus (Wild, 1988). Moreover, dorsal and ventral TO differ concerning the morphology of the outer retinorecipient as well as the deep output layers (Angaut & Repérant, 1976; Repérant & Angaut, 1977). Hayes & Webster (1985) described a shift in the thickness of the retinorecipient layers 2 to 7, most obvious in layer 5 with an increase in thickness from dorsal to ventral parts. Additionally, dorso-ventral differences in the optic terminal density in layers 2 to 7, as well as in the number of synaptic contacts per terminal were reported (Acheson *et al*., 1980; Duff *et al*., 1981). Recent experiments indicate that the retinal input to tectal layer 5 arises almost exclusively from very small retinal ganglion cells, which were shown to terminate predominantly within the ventral TO (Karten *et al*., 1997). A dorso-ventral differentiation was also demonstrated for the efferent layer 13 with the ventral TO exhibiting a twofold increase in cell number compared with the dorsal TO (Theiss *et al*., 1998). This difference might be caused by the uneven distribution of a subclass of layer 13 neurons (type I), characterized by extensive dendritic ramifications within retinorecipient layer 5 (Karten *et al*., 1997). Thickness differences of layer 5 do not increase continuously from dorsal to ventral areas. Instead, they arise in a small transition zone within the lateral TO. When mapped onto a two-dimensional reconstruction of the tectal surface, it is obvious that this transition zone almost exactly corresponds to the borderline of tectal tracer spread, resulting in either the first or second anterograde rotundal labelling pattern (Fig. 14). Tectal injections resulting in weak rotundal labelling were always located dorsally to the transition zone, while strong rotundal projections resulted from injections, situated below this region or including the transition area. Thus, the differential contribution of the dorsal and ventral TO to the tectofugal projection coincides with the distinct projection of small retinal ganglion cells onto the TO and the differential distribution of one subclass of tectofugal neurons, receiving probably monosynaptic input from these retinal afferents.

As the dorso-ventral shift in the distribution of one subclass of tectal layer 13 neurons in the pigeon generally coincides with the

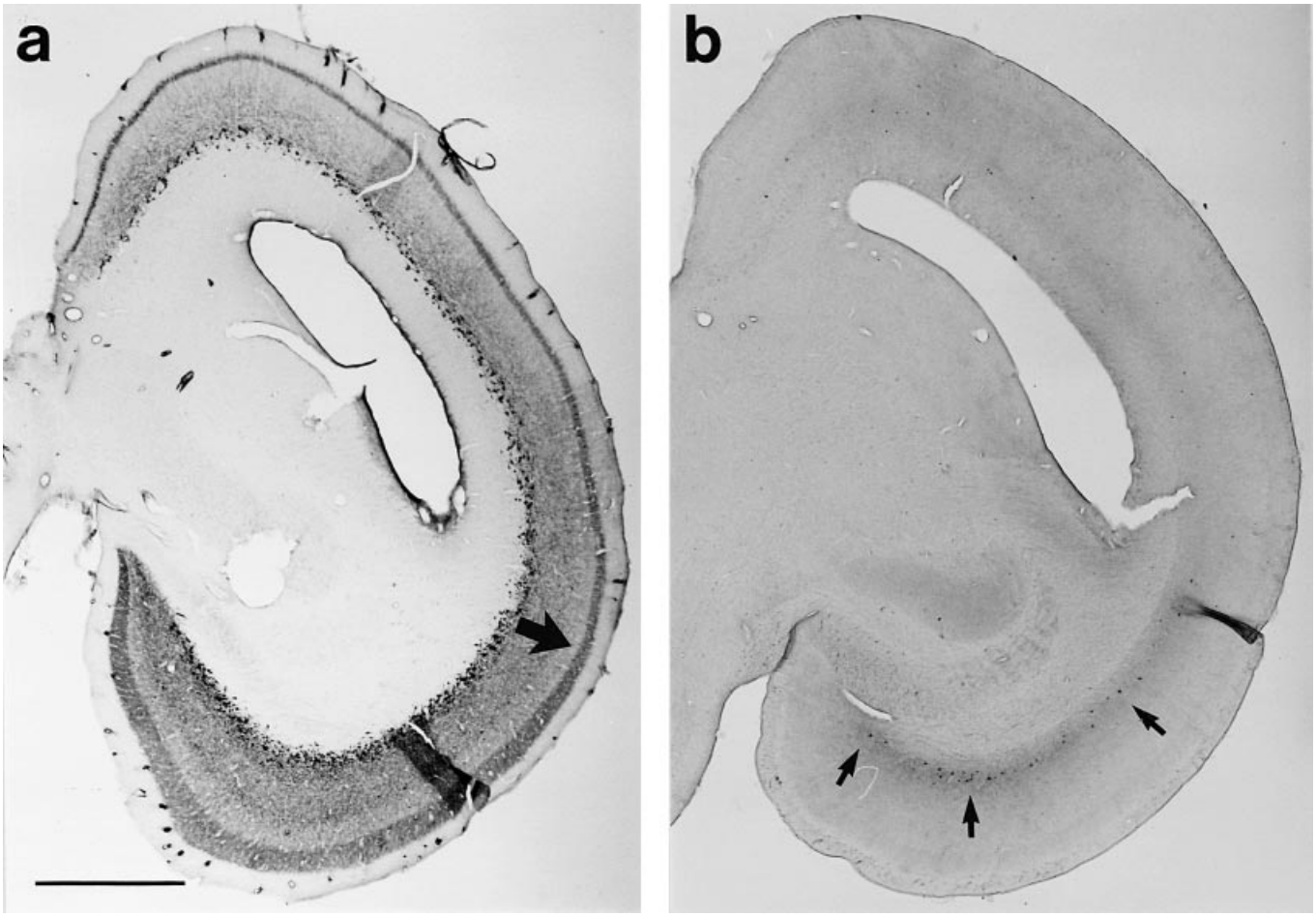

FIG. 9. Retrograde labelling of tectal layer 13 neurons after rotundal CtB (a: A2.2) and BDA (b: A2.5) injections. Retrograde CtB tracing was generally stronger compared with BDA (arrows in b), apparent in many more labelled somata and additional tracing of dendritic processes within layer 5 (arrow in a). Cell number generally increased from dorsal to ventral. After BDA applications, lateral and dorsal layer 13 neurons exhibited only very weak somatic labelling. Bar, 1000 μm.

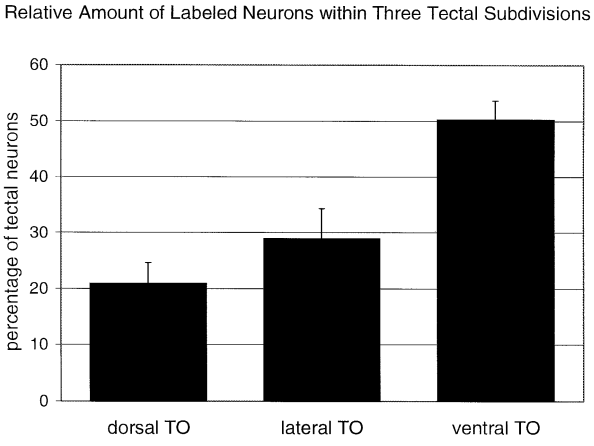

FIG. 10. Relative amount of retrogradely labelled tectal layer 13 somata within three tectal subdivisions after rotundal tracer injections ($n = 6$). Bars, standard deviations.

slighter contribution of the dorsal TO to tectofugal output, this cannot account for the clear intrarotundal regionalization of afferent input from the dorsal and ventral TO. While the most caudal tenth of the Rt was characterized by a central region of projections from the ventral TO which was surrounded by strong dorsal tectal input, this pattern reversed in the directly rostrally adjoining Rt. Here, the area of strong input from the dorsal TO gradually decreased and the rostral third was almost entirely dominated by ventral tectal input. Rotundal CtB injections revealed the neurons projecting to the central and anterior Rt to be located within the outer tectal layer 13 (Benowitz & Karten, 1976). These cells appear to constitute the type I population (Karten *et al*., 1997). In contrast, neurons of the inner sublayer project onto the T and caudal Rt (Benowitz & Karten, 1976; Deng & Rogers, 1998). These cells were shown to be equally distributed along the dorso-ventral extent of TO (Karten *et al*., 1997). The anterograde rotundal tracing data presented in this study clearly show that the intrarotundal segregation of dorsal and ventral tectal projections does not follow the regionalization in the distribution of different subclasses of layer 13 neurons in the pigeon TO. This is due to the fact that rotundal regions, defined by input from specified layer 13 sublaminae (e.g. caudal-most Rt, central Rt as well as T) exhibit internal segregation with domains of dorsal versus ventral tectal input.

The complex pattern of intrarotundal segregation, observed in the anterograde tracing experiments, might be explained by each layer 13 sublamina exhibiting an internal topography in its projection onto Rt. The retrograde tracing pattern resulting after rotundal tracer injections partly supports this view. CtB injections

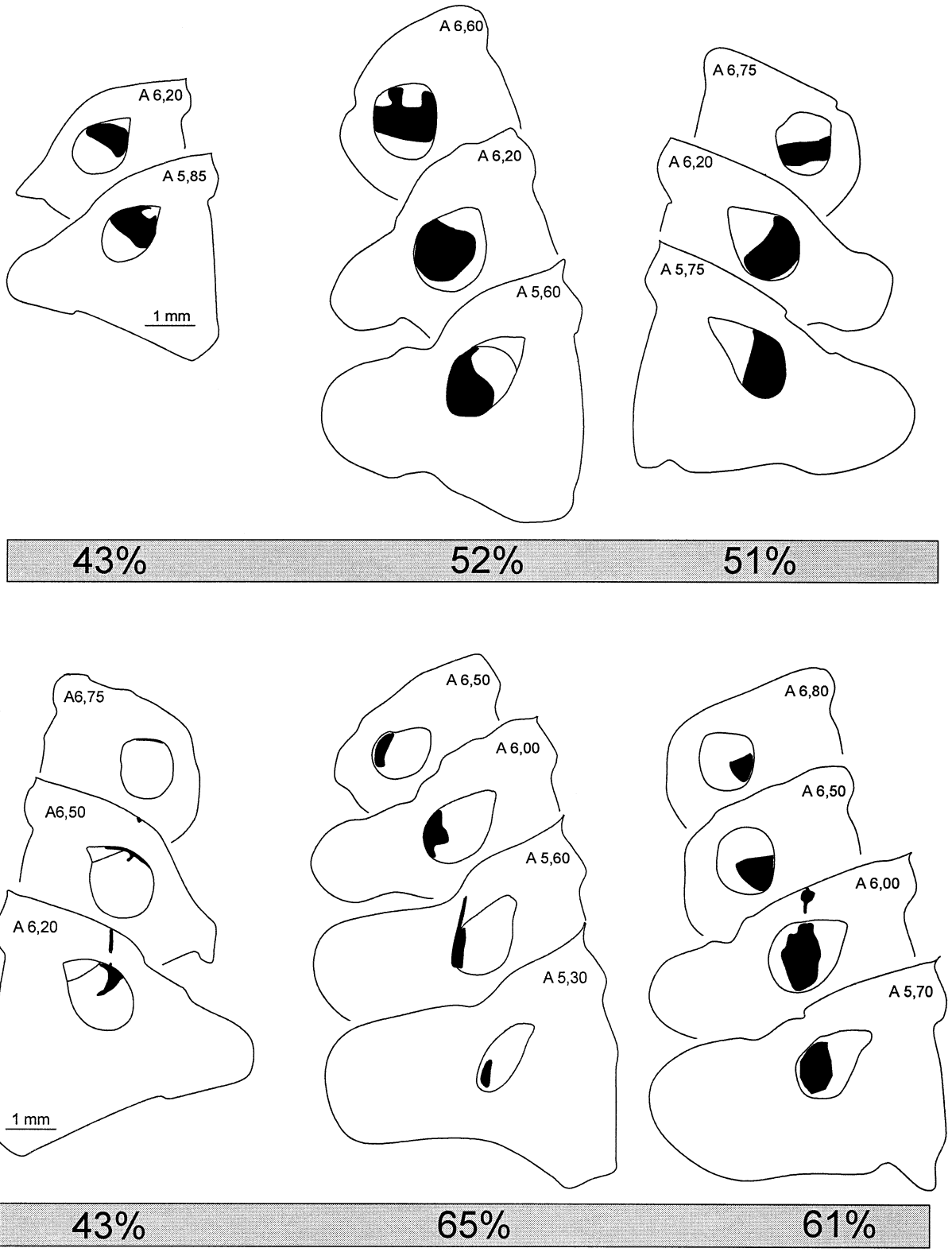

FIG. 11. Reconstruction of rotundal tracer spread (black areas) in six birds which received either CtB or BDA injections, and respective percentage of retrogradely labelled layer 13 neurons within the ventral third of the TO. The lowest percentages (both 43%) occurred in animals with tracer spread concentrated to regions which were shown to receive predominately dorsal tectal input.

into different rotundal locations resulted in labelling of tectal layer 13 neurons, concentrated to particular sublayers, depending on the respective injection site (Fig. 12). Additionally, a dorso-ventral shift in the number of traced somata was observed. So far, the results confirm earlier findings from rotundal HRP (Benowitz & Karten, 1976) or CtB injections (Karten *et al.*, 1997). BDA

injections into Rt resulted in a qualitatively corresponding labelling pattern. On the other hand, the number of retrogradely labelled layer 13 somata was remarkably reduced (to 1/15) compared with CtB injections. This reduction in cell number made it possible to plot the location of BDA-labelled somata onto a two-dimensional reconstruction of the tectal layer 13 surface. In doing so, distinct regional variations in the distribution of neurons, depending on their location in different layer 13 sublaminae, were observed (Fig. 13). This arrangement occurred in all BDA-injected animals despite varying application sites. This classification of layer 13 neurons is based exclusively on their position in different depths and does not take into account any morphological peculiarities, as morphological characterization of different lamina 13 subclasses is far from complete (Karten *et al*., 1997; Luksch *et al*., 1998), and retrograde neuronal labelling with BDA poorly reveals details, e.g. cellular processes in comparison with CtB (see above). Nevertheless, retrograde tracing data support the assumption, initially based on the anterograde tracing experiments, that different tectal layer 13 sublaminae exhibit independent topographies in their projection onto Rt.

The quantitative difference in overall rotundal fibre densities, observed after ventral in comparison with dorso-lateral tectal BDA

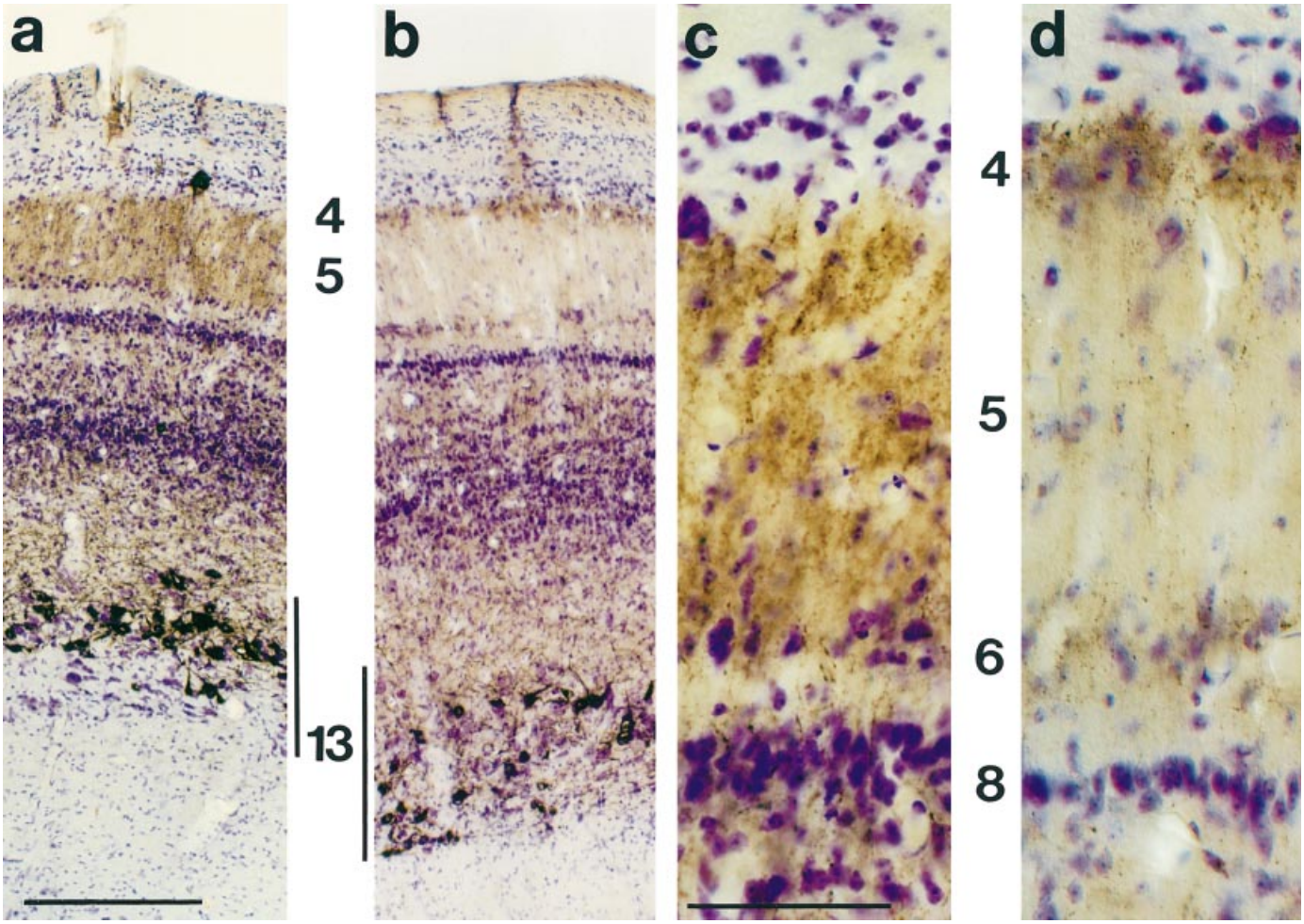

FIG. 12. Tectal coronal sections of pigeons which received CtB injections into either the rostral (a and c) or caudo-dorsal (b and d) Rt. Black to brown labelling indicates the reaction product of retrogradely transported CtB, while blue/red colour is due to cresyl violet staining of somata. Numbers indicate classification of tectal laminae according to Ramon y Cajal (1911). Rostral rotundal CtB injections resulted in tracing of tectal somata concentrated within the outer regions of layer 13 (a: 13). Dendritic tracing within the outer retinorecipient layers was concentrated to layer 5 (a and c: 5). In contrast, caudo-dorsal rotundal tracer injection resulted in somatic labelling throughout the entire layer 13 (b: 13), and dendritic staining which was concentrated in the thin lamina 4 (d: 4), while layer 5 exhibited only very weak label (d: 5). Bars, 200 µm (a and b) and 50 µm (c and d), respectively.

FIG. 13. Reconstructions of the distribution of retrogradely labelled tectal layer 13 neurons after three BDA injections (a–c) into Rt. On the left side, serial reconstructions of coronal sections indicate the location of rotundal BDA spread (black areas). The middle and left side show reconstructions of the corresponding ipsilateral tectal layer 13 surface, drawn as two-dimensional flat mounts independently for inner, central and outer layer 13. X-axis numbers indicate rostro-caudal location corresponding to the pigeon brain atlas (Karten & Hodos, 1967). Y-axis numbers indicate the dorso-ventral extension of the sublaminae. Here, only D–V 5.0 corresponds to the pigeon brain atlas, while all other numbers indicate the dorsal (positive) or ventral (negative) position relative to this anchor point. Dots drawn within these reconstructions indicate locations of layer 13 neurons. Stippled lines indicate the proposed tectal representation of the retinal central fovea (middle) and red field (lower right). Solid lines within the two-dimensional reconstructions indicate the location of the layer 5 transition zone (see arrow in Fig. 9a). The diagram indicates sublamina-specific distributions of layer 13 neurons. Cells within the inner layer were always concentrated within the ventral TO, while layer 13 neurons within the intermediate and outer sublaminae exhibited varying distributions depending on rotundal injection site. D, dorsal; V, ventral; A, anterior; P, posterior.

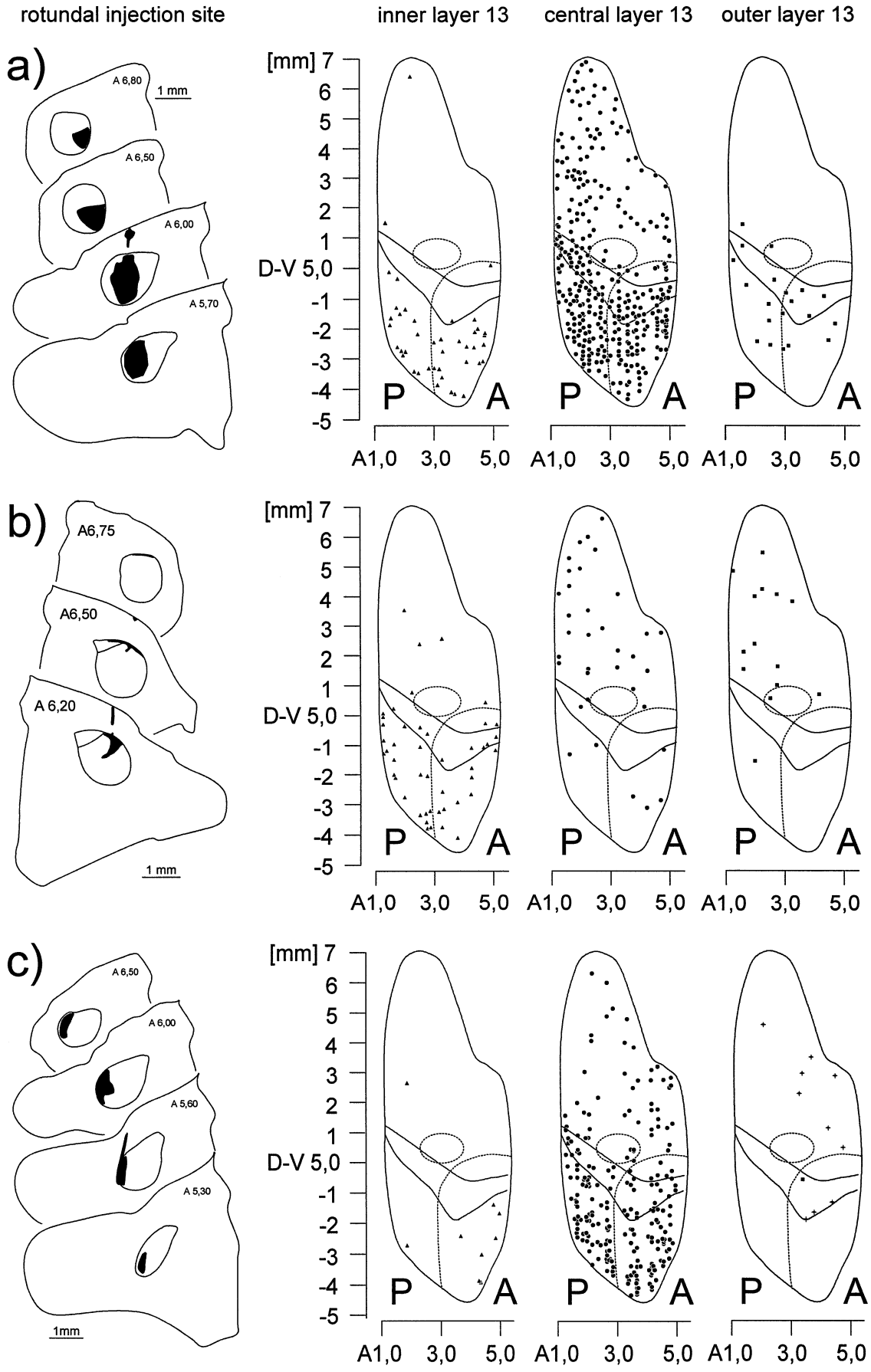
rotundal injection site
inner layer 13
central layer 13
outer layer 13
a)
A 6,80
1 mm
A 6,50
A 6,00
A 5,70
[mm] 7
6
5
4
3
2
1
D-V 5,0
-1
-2
-3
-4
-5
P
A
A1,0
3,0
5,0
b)
A6,75
A6,50
A 6,20
1 mm
c)
A 6,50
A 6,00
A 5,60
A 5,30
1mm

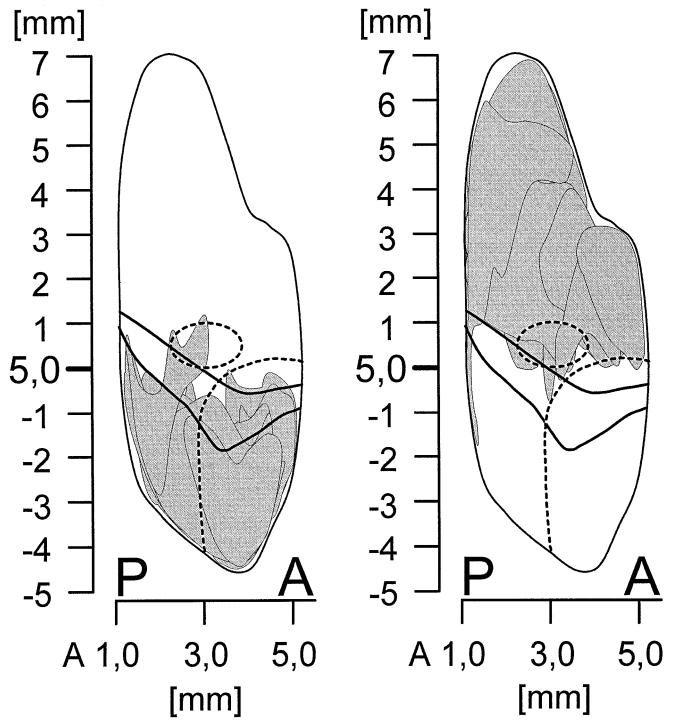

FIG. 14. Summary of tectal tracer injections and the resulting anterograde rotundal tracing patterns. For each tectal injection, the area of labelled layer 13 neurons is drawn grey onto two-dimensional reconstructions of the TO (for preparation of reconstruction see Fig. 13 legend). The left side summarizes injections which resulted in the first (strong) rotundal labelling pattern (see Fig. 3), while the right side shows the extent of injections which lead to the second (weaker) rotundal labelling pattern. Weak rotundal projections were always observed when injections were situated above the layer 5 transition zone (solid lines). In contrast, strong rotundal projections always enclosed regions below the transition zone.

injections corresponds qualitatively to the dorso-ventral shift in tectal layer 13 cell number after rotundal BDA or CtB injections. However, the rotundal fibre density index indicates that the ventral tecto-rotundal projection is 15 times larger than the dorso-lateral one, while the retrograde tracing data only indicate a twofold increase in rotundal neurons projecting from ventral TO compared with lateral and dorsal ones. This difference could be caused by a differential amount of axonal branching of layer 13 neurons, depending on their tectal location. The results from rotundal BDA injections support this point of view, as retrogradely labelled neurons within the dorsal TO always exhibited only very weak labelling just above background levels, while ventrally located somata showed clearly enhanced labelling. The difference in magnitude of retrogradely transported BDA is probably due to a dissimilar rate of tracer uptake, depending on the overall surface of axonal processes of individual neurons in the area of tracer spread. This surface-dependent effect on somatic labelling amount should be less dramatic when using more sensitive tracers with increased uptake rates or higher affinity to active axonal transport (Güntürkün *et al*., 1993a). Compared to BDA, CtB is much more effective in retrograde neuronal labelling, as rotundal applications resulted in a 15-fold increase in the number of labelled tectal somata. Indeed, dorsally located layer 13 neurons do not obviously differ in CtB labelling intensity from ventral cells. Thus, the comparison of retrograde labelling with different neuronal tracers supports the assumption of enhanced axonal branching and/or the terminal surface of ventral tectal layer 13 neurons within the Rt.

Functional considerations

Rotundal neurons show region-specific variations in their physiological properties in terms of the shape of receptive fields (Maxwell & Granda, 1979), the directional tuning (Kimberly *et al*., 1971; Maxwell & Granda, 1979; Revzin, 1979), and the general discharge patterns (Granda & Yazulla, 1971). Intrarotundal functional subdivisions were observed for wavelength preferences and colour-opponent units (Yazulla & Granda, 1973), as well as for luminance, colour, looming and motion processing (Wang & Frost, 1992; Wang *et al*., 1993). The latter authors subdivided the Rt into a ventral motion-sensitive region, a caudo-dorsal area with most units sensitive for object motion in three dimensions, and a rostro-dorsal region with a majority of luminance- and colour-sensitive cells. Because the Rt exhibits functional domains, the regionalized projections of the dorsal and ventral TO might point to visual field-dependent processing of stimulus features within the tectofugal pathway. Comparing the electrophysiologically defined subdivisions with the anterograde labelling pattern after tectal tracer injections, it is obvious that one region of strong dorsal tectal input, the dorso-central region within the caudal two-thirds of the Rt, fits with parts of the rotundal looming domain. In contrast, ventral as well as rostro-dorsal subdivisions, characterized by processing mainly motion in two dimensions, luminance and colour, receive only very weak input from the dorsal TO. Our retrograde CtB data indicate a specific projection of type III layer 13 neurons onto the dorso-central Rt, while ventral adjoining rotundal regions, possibly two-dimensional motion sensitive, receive in particular type I input (Karten *et al*., 1997). Type I as well as type III neurons share features in their morphology, e.g. large dendritic fields in combination with wide-interval dendritic endings, which suit them both to constitute elements in object motion detection networks (Luksch *et al*., 1998). Therefore, the distinct projection of these two cell types onto neighbouring rotundal areas indeed indicate that: (i) these regions are principally involved in motion processing; and (ii) there is a differential functional role of these areas in motion processing, e.g two-dimensional versus three-dimensional motion analysis. In this respect it is noteworthy that our anterograde tracing data indicate a contribution of the dorsal TO only to one rotundal motion domain, while the ventral TO projects onto both regions.

As yet, there seems to exist no physiological characterization of the caudal-most part of the Rt. Compared to the directly rostral adjoining Rt, this region receives a mirror-image-like input from tectal subfields. Moreover, Karten *et al*. (1997) suggested that the caudal Rt is innervated by type II layer 13 afferents, while the rostral adjoining Rt receives input from type I and type III neurons (see above). On the basis of the distinct innervation patterns, we suppose that the caudal Rt differs functionally from neighbouring regions. As this is the only rotundal subfield which is dominated by dorsal tectal input, its physiological characterization might help to elucidate the functional significance of visual field-specific processing within the ascending tectofugal pathway.

The T is characterized by a complex pattern of segregated input from the dorsal and ventral TO. In contrast to the rotundo-telencephalic projection, the ascending triangular projection is not organized topographically as it covers all parts of the ectostriatum (Benowitz & Karten, 1976; Nixdorf & Bischof, 1982). Therefore, we suggest a modulatory role for the nucleus triangularis in tectofugal information processing, depending on inputs from the dorsal as well as ventral TO.

The anterograde tracing data presented in this paper reveal a differential contribution of different tectal regions in tectofugal information processing. Because of the topographic arrangement of the retino-tectal projection, they also indicate visual field-specific alterations in tectofugal information processing. As the Rt is characterized by the formation of various functional domains, the regionalized and segregated projections of dorsal and ventral TO additionally indicate visual field-dependent analysis of stimulus features. The borderline between the two tectal projection patterns exactly matches the transition zone of retinorecipient layer 5, indicating that the dorso-ventral distinction within the tectofugal pathway runs along the horizontal meridian of the visual field (Hamdi & Whitteridge, 1954; Remy & Güntürkün, 1991). On the other hand, Karten *et al*. (1997) stated that small retinal ganglion cells, which seem to terminate specifically within tectal layer 5, are predominantly concentrated within the retinal area dorsalis, the frontal visual field representation. Karten *et al*. concluded that tectal layer 5 regionalization reflects the retinal red/yellow field differentiation, which indicates a somehow different retino-tectal topography (see also Jassik-Gerschenfeld & Hardy, 1984). Irrespective of whether the differentiation in tectofugal information processing concerns the horizontal meridian or more specifically the frontal/lateral visual field distinction, it points to a quantitatively strongly enhanced contribution of the lower frontal visual field within ascending tectofugal processes. Thus, the anatomical data on tecto-rotundal connectivities presented here, indeed constitute a possible anatomical basis for the recent observation of visual field-specific behavioural effects of Rt and GLd lesions (Güntürkün & Hahmann, 1998), discussed in the Introduction. The thalamofugal and tectofugal pathway seem to be organized in a complementary pattern, with the GLd receiving visual input mainly from retinal ganglion cells of the lateral (yellow) visual field (Remy & Güntürkün, 1991) and the Rt, being dominated by inputs from the frontal (red) visual field. This fundamental dichotomy in visual information processing within the pigeon is first notable within the eye, with the differentiation in the myopic lower visual field (Bloch & Martinoya, 1983; Fitzke *et al*., 1985), the differential distribution of wavelength-sensitive photoreceptors (Remy & Emmerton, 1989), the uneven and cell type-specific distribution of retinal ganglion cells (Hayes *et al*., 1987; Karten *et al*., 1997), and the differential rates of intraocular transfer between red and yellow field (Remy & Emmerton, 1991). So, visual field-dependent specializations, as shown here for the tecto-rotundal projection, seem to be a general principle in the pigeon's visual system.

Acknowledgements

We wish to thank Ariane Schwarz for excellent technical assistance, Martina Manns for many helpful discussions, and Drs Helmut Prior and Markus M. Schugens for critical reading of the manuscript. This research was supported by grants from the Deutsche Forschungsgemeinschaft (Gu 227/4-2/3 and Sonderforschungsbereich 509 NEUROVISION) and the Alfried Krupp-Stiftung.

Abbreviations

BDA, biotinylated dextran amine; CtB, choleratoxin subunit B; DAB, 3,3′-diaminobenzidine; FDA, fluorescein dextran amine; GLd, nucleus geniculatus lateralis, pars dorsalis; HRP, horseradish peroxidase; PB, phosphate buffer; PBS, phosphate-buffered saline; PV, nucleus posteroventralis thalami; Rt, nucleus rotundus; T, nucleus triangularis; TDA, Texas Red dextran amine; TO, tectum opticum.

References

Acheson, D.W., Kemplay, S.K. & Webster, K.E. (1980) Quantitative analysis of optic terminal profile distribution within the pigeon optic tectum. *Neuroscience*, **5**, 1067–1084.

Adams, J.C. (1981) Heavy metal intensification of DAB-based HRP reaction product. *J. Histochem. Cytochem.*, **29**, 775.

Angaut, P. & Repérant, J. (1976) Fine structure of the optic fibre termination layers in the pigeon optic tectum: a Golgi and electron microscope study. *Neuroscience*, **1**, 93–105.

Bagnoli, P. & Burkhalter, A. (1983) Organization of the afferent projections to the wulst in the pigeon. *J. Comp. Neurol.* **214**, 103–113.

Benowitz, L.I. & Karten, H.J. (1976) Organization of tectofugal visual pathway in pigeon: retrograde transport study. *J. Comp. Neurol.*, **167**, 503–520.

Bessette, B.B. & Hodos, W. (1989) Intensity, color, and pattern discrimination deficits after lesions of the core and the belt regions of the ectostriatum. *Vis. Neurosci.*, **2**, 27–34.

Bischof, H.J. & Niemann, J. (1990) Contralateral projection of the optic tectum in the zebra finch (*Taenopygia guttata castanotis*). *Cell Tissue Res.*, **262**, 307–313.

Bloch, S. & Martinoya, C. (1983) Specialization of visual functions for different retinal areas in the pigeon. In Ewert, J.-P., Capranica, R.R. & Ingle, D.J. (eds), *Advances in Vertebrate Neuroethology*. Plenum Press, New York, pp. 359–368.

Bravo, H. & Inzunza, O. (1983) Estudio anatomico en las vias visuales parallelas en falconiformes. *Arch. Bio. Med. Exp.*, **16**, 283–289.

Bravo, H. & Pettigrew, J. (1981) The distribution of neurons projecting from the retina and visual cortex to the thalamus and tectum opticum of the barn owl, Tyto alba, and the burrowing owl, Speotyto cunicularia. *J. Comp. Neurol.*, **199**, 419–441.

Britten, K.H. (1987) *Receptive Fields of Neurons of the Principal Optic Nucleus of the Pigeon (Columba livia).* Sunny, Stony Brook.

Britto, L.R., Brunelli, G., Francesconi, W. & Magni, F. (1975) Visual response pattern of thalamic neurons in the pigeon. *Brain Res.*, **97**, 337–343.

Deng, C. & Rogers, L.J. (1998) Organisation of the tectorotundal and SP/IPS-rotundal projections in the chick. *J. Comp. Neurol.*, **394**, 171–185.

Duff, T.A., Scott, G. & Mai, R. (1981) Regional differences in pigeon optic tract, chiasm, and retino-receptive layers of optic tectum. *J. Comp. Neurol.*, **198**, 231–247.

Fitzke, F.W., Hayes, B.P., Hodos, W., Holden, A.L. & Low, J.C. (1985) Refractive sectors in the visual field of the pigeon eye. *J. Physiol.,* (*Lond.*), **369**, 33–44.

Frost, B.J. & DiFranco, D.E. (1976) Motion characteristics of single units in the pigeon optic tectum. *Vision Res.*, **16**, 1229–1234.

Gamlin, P.D., Reiner, A., Keyser, K.T., Brecha, N. & Karten, H.J. (1996) Projection of the nucleus pretectalis to a retinorecipient tectal layer in the pigeon (Columba livia). *J. Comp. Neurol.*, **368**, 424–438.

Granda, A.M. & Yazulla, S. (1971) The spectral sensitivity of single units in the nucleus rotundus of pigeon, Columba livia. *J. Gen. Physiol.*, **57**, 363–384.

Güntürkün, O. & Hahmann, U. (1999) Functional subdivisions of the ascending visual pathways in the pigeon. *Brain Res.* (in press).

Güntürkün, O., Melsbach, G., Hörster, W. & Daniel, S. (1993a) Different sets of afferents are demonstrated by the two fluorescent tracers Fast Blue and Rhodamine. *J. Neurosci. Meth.*, **49**, 103–111.

Güntürkün, O., Miceli, D. & Watanabe, M. (1993b) Anatomy of the avian thalamofugal pathway. In Zeigler, H.P. & Bischof, H.-J. (eds), *Vision, Brain and Behavior in Birds.* MIT press, Cambridge, MA, pp. 115–135.

Hamdi, F.A. & Whitteridge, D. (1954) The representation of the retina on the optic tectum of the pigeon. *Q. J. Exp. Psychol.*, **39**, 111–119.

Hayes, B.P., Hodos, W., Holden, A.L. & Low, A.L. (1987) The projection of the visual field upon the retina of the pigeon. *Vision Res.*, **27**, 31–40.

Hayes, B.P. & Webster, K.E. (1985) Cytoarchitectural fields and retinal termination: an axonal transport study of laminar organization in the avian optic tectum. *Neuroscience*, **16**, 641–657.

Hodos, W. (1969) Color-discrimination deficits after lesions of the nucleus rotundus in pigeons. *Brain Behav. Evol.*, **2**, 185–200.

Hodos, W. (1976) Vision and the visual system: A bird's eye view. In Sprague, J.M. & Epstein, A.N. (eds), *Progress in Psychobiology and Physiological Psychology*, Vol. 6. Academic Press, New York, pp. 29–62.

Hodos, W. & Bonbright, J.C. (1974) Intensity difference thresholds in pigeons after lesions of the tectofugal and thalamofugal visual pathways. *J. Comp. Physiol. Psychol.*, **87**, 1013–1031.

Hodos, W. & Karten, H.J. (1966) Brightness and pattern discrimination deficits after lesions of nucleus rotundus in the pigeon. *Exp. Brain Res.*, **2**, 151–167.

Hunt, S.P. & Künzle, H. (1976) Observations on the projections and intrinsic

organization of the pigeon optic tectum: an autoradiographic study based on anterograde and retrograde, axonal and dendritic flow. *J. Comp. Neurol.*, **170**, 153–172.
Jassik-Gerschenfeld, D. & Guichard, J. (1972) Visual receptive fields of single cells in the pigeon's optic tectum. *Brain Res.*, **40**, 303–317.
Jassik-Gerschenfeld, D. & Hardy, O. (1984) The avian optic tectum: neurophysiology and behavioural correlations. In Vanegas, H. (ed.), *Comparative Neurology of the Optic Tectum*. Plenum Press, New York, pp. 649–686.
Jassik-Gerschenfeld, D., Teulon, J. & Ropert, N. (1976) Visual receptive field types in the nucleus dorsolateralis anterior of the pigeon's thalamus. *Brain Res.*, **108**, 295–306.
Karten, H.J., Cox, K. & Mpodozis, J. (1997) Two distinct populations of tectal neurons have unique connections within the retinotectorotundal pathway of the pigeon (Columba livia). *J. Comp. Neurol.*, **387**, 449–465.
Karten, H.J. & Hodos, W. (1967) *A Stereotaxic Atlas of the Brain of the Pigeon.* The Johns Hopkins Press, Baltimore.
Karten, H.J. & Hodos, W. (1970) Telencephalic projections of the nucleus rotundus in the pigeon (Columba livia). *J. Comp. Neurol.*, **140**, 35–52.
Karten, H.J., Nauta, W.J.H. & Revzin, A.M. (1973) Neural connections of the 'visual wulst' of the avian telencephalon. Experimental studies in the pigeon (Columba livia) and owl (Speotyto cunicularia). *J. Comp. Neurol.*, **150**, 253–278.
Karten, H.J. & Revzin, A.M. (1966) The afferent connections of the nucleus rotundus in the pigeon. *Brain Res.*, **2**, 368–377.
Kimberly, R.P., Holden, A.L. & Bamborough, P. (1971) Response characteristics of pigeon forebrain cells to visual stimulation. *Vision Res.*, **11**, 475–478.
Luksch, H., Cox, K. & Karten, H.J. (1998) Bottlebrush dendritic endings and large dendritic fields: Motion-detecting neurons in the tectofugal pathway. *J. Comp. Neurol.*, **396**, 399–414.
Martinez-de-la-Torre, M., Martinez, S. & Puelles, L. (1990) Acetylcholinesterase-histochemical differential staining of subdivisions within the nucleus rotundus in the chick. *Anat. Embryol.*, **181**, 129–135.
Maxwell, J.H. & Granda, A.M. (1979) Functional localization in the nucleus rotundus. In Granda, A.M. & Maxwell, J.H. (eds), *Neural Mechanisms of Behavior in the Pigeon.* Plenum Press, New York, pp. 177–197.
Miceli, D., Gioanni, H., Repérant, J. & Peyrichoux, J. (1979) The avian visual wulst: I. An anatomical study of afferent and efferent pathways. II. An electrophysiological study of the functional properties of single neurons. In Granda, A.M. & Maxwell, J.H. (eds), *Neural Mechanisms of Behavior in the Pigeon.* Plenum Press, New York, pp. 223–254.
Miceli, D., Marchand, L., Repérant, J. & Rio, J.-P. (1990) Projections of the dorsolateral anterior complex and adjacent thalamic nuclei upon the visual wulst in the pigeon. *Brain Res.*, **518**, 317–323.
Mulvanny, P. (1979) Discrimination of the line orientation by visual nuclei. In Granda, A.M. & Maxwell, J.H. (eds), *Neural Mechanisms of Behavior in the Pigeon.* Plenum Press, New York, pp. 199–222.
Ngo, T.D., Davies, D.C., Egedi, G.Y. & Tömböl, T. (1994) A phaseolus lectin anterograde tracing study of the tectorotundal projections in the domestic chick. *J. Anat.*, **184**, 129–136.
Nixdorf, B.E. & Bischof, H.J. (1982) Afferent connections of the ectostriatum and visual wulst in the zebrafinch (Taeniopygia guttata castanotis Gould) – an HRP study. *Brain Res.*, **248**, 9–17.
Pritz, M.B., Mead, W.R. & Northcut, R.G. (1970) The effects of wulst ablations on color, pattern and brightness discrimination in the pigeon. *J. Comp. Neurol.*, **140**, 81–100.
Ramon y Cajal, S. (1911) *Histologie du Système Neveux de l'Homme et des Vertébrés*, Vol. 2. Maloine, Paris.
Remy, M. & Emmerton, J. (1989) Behavioral spectral sensitivities of different retinal areas in the pigeon. *Behav. Neurosci.*, **103**, 170–177.
Remy, M. & Emmerton, J. (1991) Directional dependence of intraocular transfer of stimulus detection in pigeons (Columba livia). *Behav. Neurosci.*, **105**, 647–652.
Remy, M. & Güntürkün, O. (1991) Retinal afferents to the tectum opticum and the n.opticus principalis thalami in the pigeon. *J. Comp. Neurol.*, **305**, 57–70.
Repérant, J. & Angaut, P. (1977) The retinotectal projections in the pigeon. An experimental optical and electron microscope study. *Neuroscience*, **2**, 119–140.
Revzin, A.M. (1979). Functional localization in the nucleus rotundus. In Granda, A.M. & Maxwell, J.H. (eds), *Neural Mechanisms of Behavior in the Pigeon.* Plenum Press, New York, pp. 165–176.
Shimizu, T. & Karten, H.J. (1993) The avian visual system and the evolution of the neocortex. In Zeigler, H.P. & Bischof, H.-J. (eds), *Vision, Brain and Behavior in Birds.* MIT Press, Cambridge, MA, pp. 104–114.
Shu, S.Y. (1988) The glucose oxidase-DAB-nickel method in peroxidase histochemistry of the nervous system. *Neurosci. Lett.*, **85**, 169–171.
Theiss, C., Hellmann, B. & Güntürkün, O. (1998) The differential distribution of AMPA-receptor subunits in the tectofugal system of the pigeon. *Brain Res.*, **785**, 114–128.
Thin, N.D., Egedy, G. & Tömböl, T. (1992) Golgi study on neurons and fibers in nucl. rotundus of the thalamus in chicks. *J. Hirnforsch.*, **33**, 203–214.
Tömböl, T., Ngo, T.D. & Egedy, G. (1992) EM and EM golgi study on structure of nucleus rotundus in chicks. *J. Hirnforsch.*, **33**, 215–234.
Wang, Y. & Frost, B.J. (1992) Time to collision is signalled by neurons in the nucleus rotundus of pigeons. *Nature*, **356**, 236–238.
Wang, Y., Jiang, S. & Frost, B.J. (1993) Visual processing in pigeon nucleus rotundus: luminance, color, motion, and looming subdivisions. *Vis. Neurosci.*, **10**, 21–30.
Watanabe, S. (1991) Effects of ectostriatal lesions on natural concept, pseudoconcept, and artificial pattern discrimination in pigeons. *Visual Neurosci.*, **6**, 497–506.
Watanabe, M., Ito, H. & Ikushima, M. (1985) Cytoarchitecture and ultrastructure of the avian ectostriatum: afferent terminals from the dorsal telencephalon and some nuclei in the thalamus. *J. Comp. Neurol.*, **236**, 241–257.
Wild, J.M. (1988) Vestibular projections to the thalamus of the pigeon: an anatomical study. *J. Comp. Neurol.*, **271**, 451–460.
Woodson, W., Shimizu, T., Wild, J.M., Schimke, J., Cox, K. & Karten, H.J. (1995) Centrifugal projections upon the retina: an anterograde tracing study in the pigeon (Columba livia). *J. Comp. Neurol.*, **362**, 489–509.
Yazulla, S. & Granda, A.M. (1973) Opponent-color units in the thalamus of the pigeon (Columba livia). *Vision Res.*, **13**, 1555–1563.